

Spin-Valley Optical Selection Rule and Strong Circular Dichroism in Silicene

Motohiko Ezawa

Department of Applied Physics, University of Tokyo, Hongo 7-3-1, 113-8656, Japan

Silicene (a monolayer of silicon atoms) is a topological insulator, which undergoes a topological phase transition to a band insulator under an external electric field. The spin polarization is unique and opposite at the K and K' points due to the spin-orbit coupling. Accordingly, silicene exhibits a strong circular dichroism with respect to optical absorption, obeying a certain spin-valley selection rule. It is remarkable that this selection rule is drastically different between these two types of insulators owing to a band inversion taking place at the phase transition point. Hence we can tell experimentally whether silicene is in the topological or band insulator phase by circular dichroism. Furthermore the selection rule enables us to excite electrons with definite spin and valley indices by optical absorption. Photo-induced current is spin polarized, where the spin direction is different between the topological and band insulators. It is useful for future spintronics applications.

Introduction: Silicene consists of a honeycomb lattice of silicon atoms with buckled sublattices made of A sites and B sites. The states near the Fermi energy are π orbitals residing near the K and K' points at opposite corners of the hexagonal Brillouin zone. Silicene has recently been synthesized¹⁻³ and attracted much attention⁴⁻⁷. The low-energy dynamics in the K and K' valleys is described by the Dirac theory as in graphene. However, Dirac electrons are massive due to a relatively large spin-orbit (SO) gap of 1.55meV in silicene. It is remarkable that the mass can be controlled⁶ by applying the electric field E_z perpendicular to the silicene sheet.

A novel feature is that silicene is a topological insulator⁵, which is characterized by a full insulating gap in the bulk and helical gapless edges^{8,9}. It undergoes a topological phase transition from a topological insulator to a band insulator as $|E_z|$ increases and crosses the critical field E_{cr} , as has been shown by examining numerically the emergence of the helical zero energy modes in silicene nanoribbons⁶ and also by calculating the topological numbers¹⁰. It is an intriguing problem how to detect experimentally whether an insulator is topological or not just by the bulk property.

The interaction of light with matter depends on the polarization of the photons in general. When the response of a system to the left- and right-handed circularly polarized light is different, the phenomenon is referred to as circular dichroism. The circular dichroism has been shown to be essential to analyze the valley-dependent interplay of electrons in graphene^{11,18} as well as in monolayer dichalcogenides^{12,17}.

In this paper, we investigate optical absorptions in silicene. The crucial property is the spin polarization is unique and opposite at the K and K' points due to the SO coupling for $E_z \neq 0$. Hence silicene exhibits a strong circular dichroism, where the optical absorption of circularly polarized light strongly depends on the spin and valley. Furthermore, the optical selection rules are entirely different between a topological insulator and a band insulator, as enables us to tell whether silicene is in the topological or band insulator phase. The difference originates in a band inversion taking place at the phase transition point. It is remarkable that we can detect a topological phase transition by the change of circular dichroism as $|E_z|$ crosses the critical field E_{cr} . It is also remarkable that, by irradiating right-handed circularly polarized light, for instance, we can selectively excite up spin at the K point. By ap-

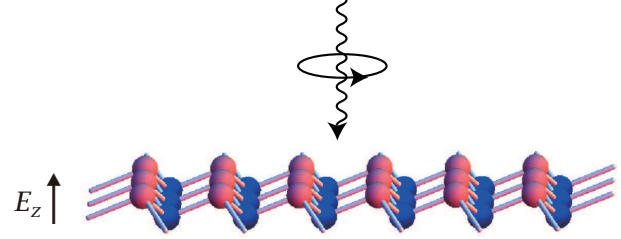


FIG. 1: (Color online) Illustration of the buckled honeycomb lattice of silicene. A honeycomb lattice is distorted due to a large ionic radius of a silicon atom and forms a buckled structure. The A and B sites form two sublattices separated by a perpendicular distance 2ℓ . The structure generates a staggered sublattice potential in the electric field E_z . Silicene undergoes a phase transition from a topological insulator to a band insulator. It is possible to discriminate between these two types of insulators by circular dichroism.

plying an in-plane electric field, photo-excited spin-polarized charges can be extracted. We can determine whether the system is topological or band insulator by detecting the spin direction of the photo-induced current.

Low-Energy Dirac Theory: We take a silicene sheet on the xy -plane, and apply the electric field E_z perpendicular to the plane. Due to the buckled structure the two sublattice planes are separated by a distance, which we denote by 2ℓ with $\ell = 0.23\text{\AA}$, as illustrated in Fig.1. It generates a staggered sublattice potential $\propto 2\ell E_z$ between silicon atoms at A sites and B sites.

We analyze the physics of electrons near the Fermi energy, which is described by Dirac electrons near the K and K' points. We also call them the K_ξ points with $\xi = \pm$. The effective Dirac Hamiltonian in the momentum space reads⁷

$$H_\xi = \hbar v_F (\xi k_x \tau_x + k_y \tau_y) + \lambda_{SO} \sigma_z \xi \tau_z - \ell E_z \tau_z + a \xi \tau_z \lambda_{R2} (k_y \sigma_x - k_x \sigma_y) + \lambda_{R1} (E_z) (\xi \tau_x \sigma_y - \tau_y \sigma_x) / 2, \quad (1)$$

where σ_a and τ_a are the Pauli matrices of the spin and the sublattice pseudospin, respectively. We explain each term. The first term arises from the nearest-neighbor hopping, where $v_F = \frac{\sqrt{3}}{2} a t = 5.5 \times 10^5 \text{m/s}$ is the Fermi velocity with the transfer energy $t = 1.6\text{eV}$ and the lattice constant $a = 3.86\text{\AA}$.

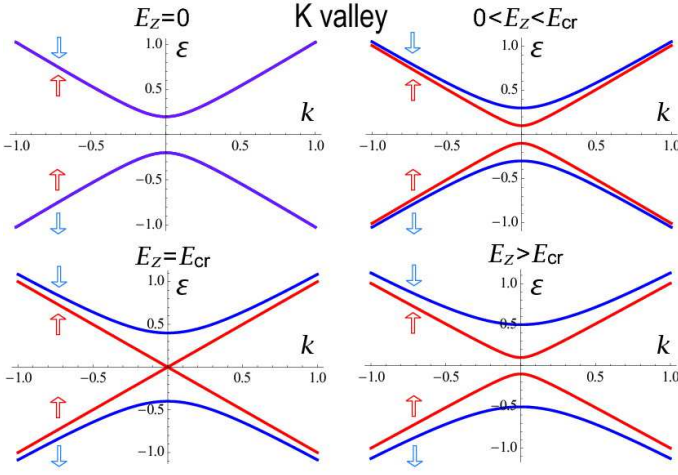


FIG. 2: (Color online) Band structure of silicene in the K valley under electric field E_z . The spins of electrons on the red (blue) band are almost up (down) polarized. They are exactly polarized if $\lambda_{R2} = 0$. Although the energy spectrum looks similar between the topological and band insulators, the pseudospin t_z is opposite at the K point. Indeed, there is a band inversion at the K point: See Fig.5. The spin direction is opposite in the K' valley. The units of the vertical and horizontal axes are arbitrary.

The second term represents the effective SO coupling^{13,14} with $\lambda_{SO} = 3.9\text{meV}$. The third term represents the staggered sublattice potential⁶ in electric field E_z . The fourth term represents the second Rashba SO coupling with $\lambda_{R2} = 0.7\text{meV}$ associated with the next-nearest neighbor hopping term¹⁴. The fifth term represents the first Rashba SO coupling associated with the nearest neighbor hopping, which is induced by external electric field^{15,16}. It satisfies $\lambda_{R1}(0) = 0$ and becomes of the order of $10\mu\text{eV}$ at the electric field $E_c = \lambda_{SO}/\ell = 17\text{meV}\text{\AA}^{-1}$. Its effect is negligible as far as we have checked. Although we include all terms in numerical calculations, in order to simplify the formulas and to make the physical picture clear, we set $\lambda_{R1}(E_z) = 0$ in all analytic formulas.

There are four bands in the energy spectrum (Fig.2). The band gap is located at the K and K' points. At these points the energy is given by

$$E(s_z, t_z) = \lambda_{SO}s_z t_z - \ell E_z t_z, \quad (2)$$

with the spin $s_z = \pm 1$ and the sublattice pseudospin $t_z = \pm 1$. They are good quantum numbers at the K and K' points. The spin s_z is an almost good quantum number even away from the K and K' points because λ_{R2} is a small quantity. On the other hand, the pseudospin t_z is strongly broken away from the K and K' points for $E_z \neq 0$.

The gap is given by $2|\Delta_s(E_z)|$ with

$$\Delta_s(E_z) = -\lambda_{SO} + s\ell E_z, \quad (3)$$

where $s = \pm 1$ is the spin-chirality. It is given by $s = \xi s_z$ when the spin s_z is a good quantum number. As $|E_z|$ increases, the gap decreases linearly, and closes at the critical point $|E_z| = E_{cr}$ with

$$E_{cr} = \pm \lambda_{SO}/\ell = \pm 17\text{meV}/\text{\AA}, \quad (4)$$

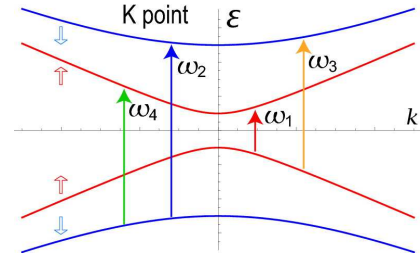


FIG. 3: (Color online) Illustration of photo-induced transition from the valence band to the conduction band at the K point. There are four ways of transitions, which we label as ω_i . The arrows ω_1 and ω_2 indicate the optical transition of high intensity proportional to v_F^2 and the arrows ω_3 and ω_4 indicate the optical transition of low intensity proportional to λ_{R2}^2 . We call the transition ω_1 as the fundamental transition.

and then increases linearly. Silicene is a semimetal due to gapless modes at $|E_z| = E_{cr}$, while it is an insulator for $|E_z| \neq E_{cr}$.

Optical properties: We explore optical interband transitions from the state $|u_v(k)\rangle$ in the valence band to the state $|u_c(k)\rangle$ in the conduction band. There are four transitions, which we label as $\omega_1, \omega_2, \omega_3$ and ω_4 , as depicted in Fig.3. We call ω_1 as the fundamental transition.

We consider a beam of circularly polarized light irradiated onto the silicene sheet. The corresponding electromagnetic potential is given by

$$\mathbf{A}(t) = (A \sin \omega t, A \cos \omega t). \quad (5)$$

The electromagnetic potential is introduced into the Hamiltonian (1) by way of the minimal substitution, that is, replacing the momentum $\hbar k_i$ with the covariant momentum $P_i \equiv \hbar k_i + eA_i$. The resultant Hamiltonian simply reads

$$H_\xi(A) = H_\xi + \mathcal{P}_x^\xi A_x + \mathcal{P}_y^\xi A_y, \quad (6)$$

with (1) and

$$\begin{aligned} \mathcal{P}_x^\xi &= \frac{1}{\hbar} \frac{\partial H_\xi}{\partial k_x} = v_F \xi \tau_x - \frac{a\lambda_{R2}}{\hbar} \xi \tau_z \sigma_y, \\ \mathcal{P}_y^\xi &= \frac{1}{\hbar} \frac{\partial H_\xi}{\partial k_y} = v_F \tau_y + \frac{a\lambda_{R2}}{\hbar} \xi \tau_z \sigma_x, \end{aligned} \quad (7)$$

since the Dirac Hamiltonian is linear in the momentum. It is notable that the formula does not contain the SO coupling λ_{SO} . We conclude from this formula that the kinetic term ($\propto v_F$) induces an interband transition between electrons carrying the same spin while the Rashba term ($\propto \lambda_{R2}$) induces an interband transition between electrons carrying the opposite spins.

The coupling strength with optical fields of the right(+) or left(-) circular polarization is given by $\mathcal{P}_\pm^\xi(k) = \mathcal{P}_x^\xi(k) \pm i\mathcal{P}_y^\xi(k)$. They are written in terms of the ladder operator of spins and pseudospins.

$$\mathcal{P}_\pm^K = v_F \tau_\pm \pm \frac{ia\lambda_{R2}}{\hbar} \tau_z s_\pm, \quad (8)$$

$$\mathcal{P}_\pm^{K'} = -v_F \tau_\mp \mp \frac{ia\lambda_{R2}}{\hbar} \tau_z s_\pm, \quad (9)$$

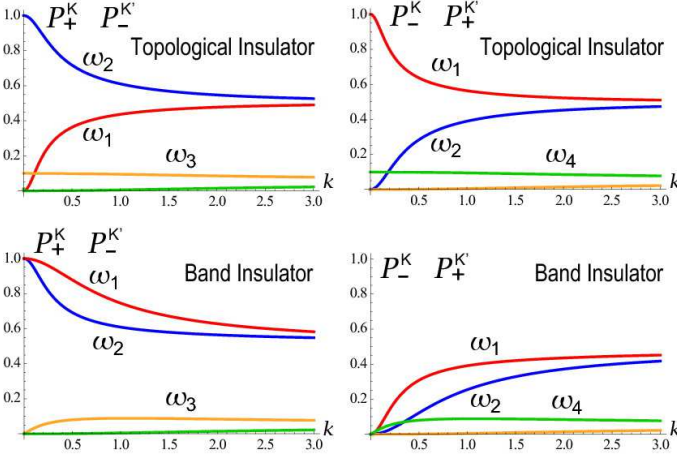


FIG. 4: (Color online) The k -resolved optical absorption $|P_{\pm}^{\xi}(k)|/m_0 v_F$ near the K and K' points. The horizontal axis is momentum k . We have chosen $E_z = E_{\text{cr}}/2$ for a topological insulator and $E_z = 2E_{\text{cr}}$ for a band insulator. Notice the behavior of the interband transition ω_1 , which changes drastically in the topological and band insulators. For illustration we have taken $a\lambda_{R2}/\hbar = 0.1v_F$, though the actual value is about $10^{-3}v_F$.

where $s_{\pm} = s_x \pm is_y$ and $\tau_{\pm} = \tau_x \pm i\tau_y$.

The matrix element between the initial state and the final state in the photoemission process is given by

$$P_{\pm}^{\xi}(k) \equiv m_0 \langle u_c(k) | \frac{1}{\hbar} \frac{\partial H_{\xi}}{\partial k_{\pm}} | u_v(k) \rangle, \quad (10)$$

where m_0 is the free electron mass. Here, $|P_{\pm}^{\xi}(k)|$ is called the optical absorption. There exist the relations,

$$P_{+}^K(k) = P_{-}^{K'}(k), \quad P_{-}^K(k) = P_{+}^{K'}(k), \quad (11)$$

reflecting the time-reversal symmetry. The right-handed circular polarization at the K point and the left-handed circular polarization at the K' point are equal.

The wave functions $|u_v(k)\rangle$ and $|u_c(k)\rangle$ are obtained explicitly by diagonalizing the Hamiltonian (1). We have calculated numerically the optical absorption $|P_{\pm}^{\xi}(k)|$ as a function of k near the K and K' points, which we display in Fig.4.

Let us investigate the optical absorption at $k = 0$ in detail, since we can obtain a clear physical picture at the K and K' points with the aid of analytical formulas. The Hamiltonian (1) is diagonal at the K and K' points with the eigenvalues given by (2) and the eigenfunctions given by $(1, 0, 0, 0)^t$ and so on. For $E_z > 0$, the order of the energy level is

$$E(-1, -1) > E(1, 1) > E(1, -1) > E(-1, 1) \quad (12)$$

for the topological insulator, and

$$E(-1, -1) > E(1, -1) > E(1, 1) > E(-1, 1) \quad (13)$$

for the band insulator. It is to be emphasized that the two bands near the Fermi level are inverted between the topological and band insulators, since the pseudospin t_z is flipped as E_z exceeds the critical point E_{cr} .

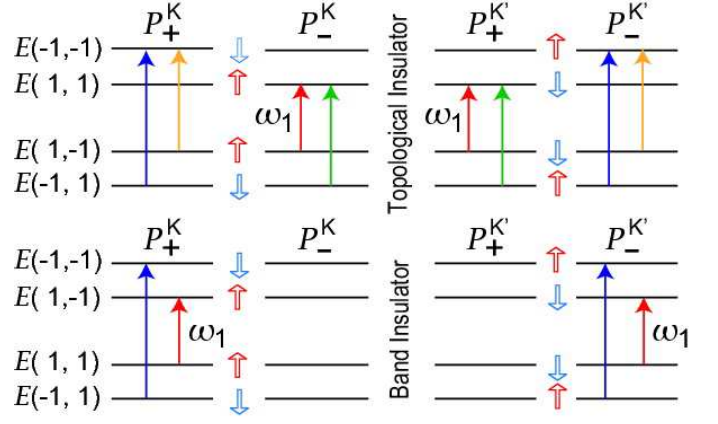


FIG. 5: (Color online) Spin-valley optical selection rules at the K and K' points ($k = 0$). The band is indexed by $E(s_z, t_z)$. The two bands $E(1, 1)$ and $E(1, -1)$ are inverted between the topological and band insulators, as leads to a different circular dichroism to them.

The band inversion leads to a different circular dichroism. This is because the operator \mathcal{P}_{\pm} is not Hermitian: \mathcal{P}_{\pm} describes an optical absorption process, while $\mathcal{P}_{\pm}^{\dagger}$ describes an optical emission process. Furthermore, an optical absorption occurs only when the energy of the initial state is lower than that of the final state. Thus the optical absorption obeys a strong spin-valley coupled selection rule (Fig.5). In conclusion, the fundamental optical absorption ω_1 (indicated by red arrow) is different whether the system is a topological insulator or a band insulator. For example, the right-circular polarized light at the K point is absorbed only when the system is a band insulator, while the left-circular polarized light at the K point is absorbed only when the system is a topological insulator. Furthermore the spin-flipped interband transitions occur only when the system is a topological insulator.

We show the optical absorption for various electric field in Fig.6. If we neglect the Rashba terms ($\lambda_{R2} = 0$) we are able to obtain an analytic formula for the transitions ω_1 and ω_2 near the K_{ξ} point,

$$\left| P_{\pm}^{\xi}(k) \right|^2 = m_0^2 v_F^2 \left(1 \pm \xi \frac{\Delta_s(E)}{\sqrt{\Delta_s^2(E) + 4a^2 t^2 k^2}} \right)^2, \quad (14)$$

where $s = +1$ for ω_1 and $s = -1$ for ω_2 . When the electric field is critical, $E_z = E_{\text{cr}}$, where $\Delta_s = 0$, the optical absorption of the fundamental transition ω_1 becomes a constant,

$$\left| P_{\pm}^{\xi}(k) \right|^2 = m_0^2 v_F^2, \quad (15)$$

which is common to the K and K' valleys. This property holds as it is even for $\lambda_{R2} \neq 0$, as seen in Fig.6.

The k -resolved optical polarization $\eta(k)$ is given by

$$\eta^{\xi}(k) = \frac{|P_{+}^{\xi}(k)|^2 - |P_{-}^{\xi}(k)|^2}{|P_{+}^{\xi}(k)|^2 + |P_{-}^{\xi}(k)|^2}. \quad (16)$$

This quantity is the difference between the absorption of the left- and right-handed lights (\pm), normalized by the total ab-

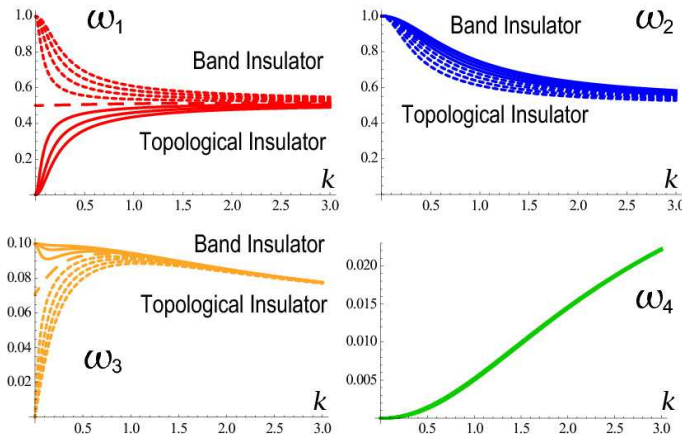


FIG. 6: (Color online) The k -resolved optical absorption $|P_+^K(k)|$ for $E_z/E_{cr} = 1/4, 1/2, 3/4, 1, 5/4, 3/2, 7/4, 2$. The solid (dotted) lines are for topological (band) insulators, while the dashed line is for the phase transition point ($E_z = E_{cr}$).

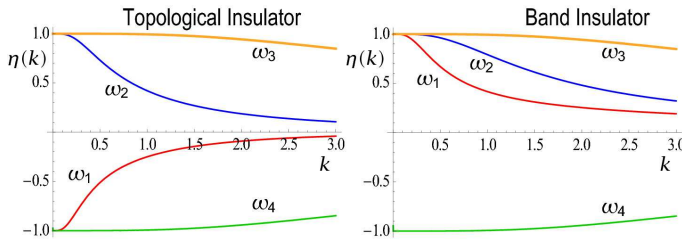


FIG. 7: (Color online) The k -resolved circular polarization $\eta(k)$ for the interband transitions ω_i in topological and band insulators.

sorption, around the K_ξ point. We show the optical polarization for the topological and band insulators in Fig.7. We find

that all optical polarizations are perfectly polarized at the K and K' points ($k = 0$). Namely, the selection rule holds exactly at the K and K' points, where $\eta = \pm 1$. Then, $|\eta^\xi(k)|$ decreases to 0 as k increases. It is to be emphasized that the optical polarization of the fundamental interband transition is opposite whether the system is a topological insulator or a band insulator.

By neglecting the Rashba term ($\lambda_{R2} = 0$), we obtain an analytic formula of the optical polarization for the transitions ω_1 and ω_2 ,

$$\eta^\xi(k) = \frac{2\xi\Delta_s\sqrt{4v_F^2k^2 + \Delta_s^2}}{4v_F^2k^2 + 2\Delta_s^2}. \quad (17)$$

The optical polarization changes the sign at the topological phase transition $E_z = E_{cr}$, since Δ_s changes the sign. This property holds as it is even for $\lambda_{R2} \neq 0$, as seen in Fig.7.

In this paper we have analyzed optical absorption in silicene. We have shown that silicene exhibits a strong circular dichroism obeying the spin-valley selection rule (Fig.5). The response is opposite whether silicene is a topological or band insulator. Indeed, in the topological (band) insulator phase, the optical field with the right-handed circular polarization excites only up-spin (down-spin) electrons in the K valley, while the one with the left-handed circular polarization excites only down-spin (up-spin) electrons in the K' valley, as far as the fundamental transition ω_1 concerns. Now, we are able to generate a longitudinal charge current with a definite spin by applying an in-plane electric field. By measuring the spin direction we can tell if silicene is a topological or band insulator.

I am very much grateful to N. Nagaosa for many helpful discussions on the subject. This work was supported in part by Grants-in-Aid for Scientific Research from the Ministry of Education, Science, Sports and Culture No. 22740196.

- ¹ P. Vogt, P. De Padova, C. Quaresima, J. A., E. Frantzeskakis, M. C. Asensio, A. Resta, B. Ealet and G. L. Lay, Phys. Rev. Lett. **108**, 155501 (2012).
- ² C.-L. Lin, R. Arafune, K. Kawahara, N. Tsukahara, E. Minamitani, Y. Kim, N. Takagi, M. Kawai, Appl. Phys. Express 5, Art No. 045802 (2012).
- ³ A. Fleurence, R. Friedlein, T. Ozaki, H. Kawai, Y. Wang, and Y. Yamada-Takamura, Phys. Rev. Lett. **108**, 245501 (2012).
- ⁴ S. Cahangirov, M. Topsakal, E. Aktürk, I H. Sahin, and S. Ciraci, Phys. Rev. Lett. **102**, 236804 (2009).
- ⁵ C.-C. Liu, W. Feng, and Y. Yao, Phys. Rev. Lett. **107**, 076802 (2011).
- ⁶ M. Ezawa, New J. Phys. **14**, 033003 (2012).
- ⁷ M. Ezawa, cond-mat/arXiv:1203.0705 (to be published in Phys. Rev. Lett.).
- ⁸ M.Z Hasan and C. Kane, Rev. Mod. Phys. **82**, 3045 (2010).

- ⁹ X.-L. Qi and S.-C. Zhang, Rev. Mod. Phys. **83**, 1057 (2011).
- ¹⁰ M. Ezawa, cond-mat/arXiv:1205.6541.
- ¹¹ W. Yao, D. Xiao, and Q. Niu, Phys. Rev. B **77**, 235406 (2008).
- ¹² D. Xiao, G.-B. Liu, W. Feng, X. Xu, and W. Yao, Phys. Rev. Lett. **108**, 196802 (2012).
- ¹³ C. L. Kane and E. J. Mele, Phys. Rev. Lett. **95**, 226801 (2005); *ibid* **95**, 146802 (2005).
- ¹⁴ C.-C. Liu, H. Jiang, and Y. Yao, Phys. Rev. B, **84**, 195430 (2011).
- ¹⁵ H. Min, J. E. Hill, N. A. Sinitsyn, B. R. Sahu, L. Kleinman, and A. H. MacDonald, Phys. Rev. B **74**, 165310 (2006).
- ¹⁶ W.K. Tse, Z. Qiao, Y. Yao, A. H. MacDonald, and Q. Niu, Phys. Rev. B **83**, 155447 (2011).
- ¹⁷ T. Cao, J. Feng, J. Shi, Q. Niu, E. Wang, cond-mat/arXiv:1112.4013.
- ¹⁸ D. Xiao, W. Yao, and Q. Niu, Phys. Rev. Lett. **99**, 236809 (2007).